

Effect Of Different Nanofluids On Solar Radiation Absorption

Suha Kareem Jebir^{†*}, Noor Yehia Abbas[‡], Ahmed F. Khudheyr^{††}

[†]Lecturer, Department of Mechanical engineering, Engineering College, Al Nahrain University, Baghdad, Iraq

[‡]Lecturer, Department of Mechanical engineering, Engineering College, Al Nahrain University, Baghdad, Iraq

^{††}Asst. Prof., Department of Mechanical engineering, Engineering College, Al Nahrain University, Baghdad, Iraq

*Corresponding Author Email: Suha.K.Jebir@ced.nahrainuniv.edu.iq

ABSTRACT: The use of solar thermal energy for water heating reduces the consumption of fossil fuels. The thermal fluids used in solar collectors have low thermal conductivity and a reduced capacity to absorb solar radiation in the visible range, where 48% of the total radiation is found. This work aims to develop various kinds of nanofluids and assess their effect on solar radiation absorption. For this reason, electron microscopy and UV-visible spectra characterize nanofluids. The thermal lead potential is measured with solar radiation obtaining the temperature profiles subjected to the nanodispersions. In addition, the effects of concentration, shape, degree of oxidation of graphene oxide (GO), the height of nanofluids are analyzed, and the properties of a hybrid nanofluid composed of GO with low oxidation with silver are evaluated. The ability to absorb visible light and the thermal conductivity of all synthesized nanofluids was enhanced compared with the deionized water. It is concluded that properties such as absorbance and transmittance do not allow evaluating the capacity for the conversion of radiation into the heat of nanofluids and the changes in these properties due to the effect of sunlight do not represent changes in the equilibrium temperature.

KEYWORDS: Nanofluids, Graphene oxide, Characterization, Solar Radiation, adsorption studies

INTRODUCTION

The study of heat transfer requires prior knowledge about the best production method and about the colloidal stability of the nanofluid in order to guarantee the proper functioning of the new exchange fluids. In addition to these, it also requires an in-depth knowledge of the thermal properties necessary for the study of heat transfer, such as thermal conductivity, specific heat, and viscosity, as these can influence the heat transfer of nanofluids. One of the pillars of the performance of solar thermal collectors is the development of new working fluids. Taking this into account, in recent decades the use of nanofluids in collectors has been evaluated because they promote greater heat removal due to their superior thermal properties compared to traditional fluids[1]. The term nanofluid was used for the first time by [2]. to define colloidal suspensions of high thermal conductivity containing particles of nanometric dimensions. The use of nanofluids as a working fluid in solar collectors for low-temperature applications has been extensively studied, revealing an increase in efficiency when compared to the use of traditional fluids such as water and ethylene glycol[3]. Heat transfer fluids such as water, mineral oil, and ethylene glycol are extremely important in many industrial processes. The weak thermal properties of conventional fluids, compared to metals, make it impossible to develop more compact and energy-efficient heat exchangers[4].

In addition to thermal applications, these fluids are useful for medical applications and catalysis in chemical reactions. However, one of the noblest uses of nanofluids is the use of their optical properties in combination with thermals for the direct conversion of solar energy through direct absorption solar collectors. Direct absorption collectors are characterized by having the working fluid in direct contact with the incident radiation, functioning as an absorber. One of the great advantages of this type of collector is that the characteristics of the nanofluid can be adjusted to obtain optical characteristics that lead to the desired absorption spectrum[5]. The need to produce fluids with superior thermal properties, coupled with the need to optimize the efficiency of conventional exchange equipment, promoted the development and investigation of new exchange fluids, including nanofluids[6]. These have numerous application possibilities, from the cooling of electronic equipment (eg computers, servers, X-ray machines, etc.), to the food, military, and aeronautical industries. The applicability of nanofluids in the solar

thermal and photovoltaic industry has also attracted a lot of interest, due to the ability of nanofluids to absorb solar radiation.[7] Despite the countless studies already carried out on this topic, there is still a great discussion about the mechanisms responsible for the heat transfer in nanofluids[8]. As mentioned earlier, nanofluids are made up of a suspension of nanoparticles in a base fluid. The addition of nanoparticles increases the thermal conductivity of conventional exchange fluids and, consequently, increases their heat transfer capacity by convection[9]. There are several studies on solar collectors where it has been shown that the replacement of conventional thermal fluids with nanofluids allows increasing thermal efficiency, for example, the study by Otanicar that shows that a 5% improvement in thermal efficiency was obtained by replacing water with nanofluids[10]. However, improvements in collector performance depend on the type of nanofluid used, the concentration of nanoparticles contained in the fluid, the shape and size of the particles, the operating conditions, among other factors[11]. In the current work, it was aimed to synthesize stable nanofluids and evaluate the effect of different nanofluids on the absorption of solar radiation.

MATERIALS AND EQUIPMENT

Materials

The materials for the synthesis of the different nanofluids correspond to analytical grade reagents purchased from Merck and Sigma Aldrich. In addition, low and high oxidation Graphene Oxide (GO) produced by the modified Hummers method[12] and silver nanoparticles in the shape of cubes were used. The water used in the synthesis of nanofluids corresponds to deionized water.

Equipment and instrumentation

Shimadzu Electronic Balance was used, which has an accuracy of $\pm 0.1 \text{ mg}$. For the preparation of the GO nanofluids, a Sonics Vibracell gun sonicator was used at 40% of its ultrasound frequency. An Elma model Transsonic 700 / H ultrasound bath was used in nanofluids stored, to characterize the nanofluids by measuring absorbance and transmittance, Elico model SL Model 159 UV-Visible spectrophotometer was used, measurements were performed using 10 mm thick quartz cuvettes and using deionized water as a reference substance. For the photothermal experiments, radiation was applied using a Sciencetech, Inc solar simulator model SF300B at an irradiance of 1000 W/m^2 by using a power of 300 W and placing the nanofluid at a distance of 180 mm from the base. To carry out the temperature measurements in the photothermal experiment, a data logger with a temperature reader, AZ Instrument brand, model AZ88598, was used, this device has four channels to connect type K thermocouples and measurements were performed every 5 seconds. To monitor the temperature during the synthesis of nanofluids, an Extech model 42509 double laser infrared thermometer was used. For the irradiance measurement of the solar simulator, a Kipp & Zonen model SP LitE2 pyranometer was used, equipped with a Kipp & Zonen Meteor data logger. To carry out the study of thermal conductivity of each nanofluid, the thermal properties analyzer brand Decagon Devices Inc. model KD2-PRO, equipped with the KS1 sensor was used. To carry out the thermal conductivity measurements, it is required that the samples to be analyzed are at a constant temperature. To achieve this, a refrigerated circulation bath, JSR model JSRC-13C, is used.

METHODOLOGY

Synthesis of nanofluids

Silver/water nanofluids

This synthesis is based on the chemical reduction method using sodium citrate[13]. Add 100 of deionized water and 19.5 g of silver nitrate (RI) to a beaker. In another beaker, place 10 g of deionized water and 10 mg of trisodium citrate (RII). RI is heated and stirred using a heating plate with a magnetic stirrer, to avoid evaporation losses the container is covered. RII is placed to shake on another magnetic plate at room temperature. When RI reaches a temperature of 90°C , RII is added by rapid dripping, it is observed that the solution begins to acquire a yellow color, it is necessary to maintain a temperature equal to or above 90°C until a dark yellow hue is reached, approximately 15 to 20 minutes counting from the moment the first drop of RII is applied. Finally, the solution is removed from the heat maintaining magnetic stirring until cool. To obtain lower concentrations of silver nanoparticles, it is diluted in deionized water until the desired concentration is reached.

Synthesis of gold/water nanofluids

This synthesis is based on the chemical reduction method using sodium citrate. In a beaker add 100 g of deionized water and 20 mg of tetrachloroauric acid (III) trihydrate (this solution is called RI). In another beaker, place 4 g of deionized water and 40 mg of trisodium citrate RII). RI is heated and stirred using a heating plate with a magnetic stirrer, to avoid evaporation losses the container is covered. RII is placed to shake on another magnetic plate at room temperature. When RI reaches a temperature of 90 ° C RII is added by rapid dripping, it is observed that seconds after applying RII the solution abruptly changes to a dark color and then acquires a reddish hue until it subsequently reaches a wine-red tint, this process takes about 10 minutes counting from the moment the first drop of RII is applied. Finally, the solution is removed from the heat maintaining magnetic stirring until cool. To obtain lower concentrations of gold nanoparticles, it is diluted in deionized water until reaching the desired concentration.

Synthesis of copper/water nanofluids

This synthesis is based on the chemical reduction method[14]. In a container, add 100 g of deionized water and 250 mg of copper sulfate pentahydrate. This solution is stirred at room temperature. Add 5 g of PVP to the solution and wait until the PVP dissolves completely. 250 mg of sodium borohydride is added, observing a color change from green, then blue to a dark brown. Keep the mixture stirring for 15 minutes counting from the moment the last reagent was added. 3.5 g of (L+) ascorbic acid is slowly incorporated and the temperature of the solution is raised to 60 ° C maintaining stirring for 30 minutes. Finally, it is removed from the heat and left stirring until cool. To obtain lower concentrations of copper nanoparticles, it is diluted using deionized water until the desired concentration is reached.

Synthesis of GO/water nanofluids

Add 100 mg GO in 100 g deionized water, then disperse using the gun sonicator for one hour. In the case of mass losses due to evaporation, the lost water is replaced. To obtain lower concentrations, it is diluted in deionized water until reaching the desired concentration. This method is the same for both low oxidation and high oxidation GO.

Synthesis of silver nanofluids-GO / water

The synthesis of silver nanofluid was performed by two methods: in situ and ex-situ. The first is based on the chemical reduction method using sodium borohydride. 2.4 mg GO is added in 25 g deionized water (this solution is called RI). The sonicator is used to disperse RI for 30 minutes. In a beaker (RII), prepare a solution of 8.7 mg of silver nitrate in 4 g of deionized water. RI is mixed with RII (this solution will be called R) and dispersed again utilizing the sonicator for 30 minutes. Then R is placed in a container and stirred magnetically. In another container (RIII), a solution of 20 mg of sodium borohydride in 10 g of deionized water is made and applied dropwise to solution R. Finally, magnetic stirring is maintained for 4 hours. For ex-situ synthesis, silver and GO nanofluids are manufactured separately and mixed in the desired proportions.

Characterization

For the determination of absorbance and transmittance of nanofluids, a UV-vis spectrophotometer was used, making measurements between wavelengths from 300 nm to 800 nm. 10 mm × 10mm × 40 mm quartz cuvettes were used and deionized water is used as a reference. The spectrum of the fluids was obtained after synthesis. For SEM and TEM images, the FESEM Quanta 250 FEG field emission cathode scanning electron microscope equipment was used. The samples were prepared on copper grids for TEM, dropping drops of a dilution of the nanofluids that were previously dispersed using a sonicator.

Stability of nanofluids over time

To study the stability of nanofluids, the absorbance spectrum is measured, using the UV-Vis spectrophotometer, at the time of synthesizing them and then after some time. To carry out the second measurement, the nanofluids were stored in a place where they were kept at rest and stored at room temperature. The cuvettes used to perform the measurements on the spectrophotometer are quartz and have measurements of 10 mm × 10mm × 40 mm. It should be noted that the reference substance corresponds to deionized water.

Photothermic experiments

For this work, a photo thermic experiment is defined as the heating of a fluid using simulated solar radiation. The experimental setup used consists of a solar simulator, a data logger with thermocouples, and the container for the nanofluid composed of a thermally insulated Petri dish and a 3 mm thick glass cover. Each nanofluid was placed in a Petri dish 45 mm in diameter and 13 mm in height, thermally insulated by a polystyrene block covered with reflective paper and covered with 3 mm thick glass. Tests were performed for two different amounts of nanofluids: mount A with 6 g and mount B with 20 g. For the first, the fluid reached a height of 4 mm, while for the second it reached 13 mm. Mount B was only used to study the effect of nanofluid height on radiation absorption. Two K-type thermocouples were placed at 3 mm in height concerning the bottom of the Petri dish to monitor the temperature in the nanofluid and a thermocouple outside the system to measure the ambient temperature, the temperature data were stored by means of a data logger. The container is placed under the solar simulator lamp at an irradiance of $1,000 \text{ W} / \text{m}^2$ for 50 minutes.

Stability of nanofluids subjected to radiation

To study the stability of the nanofluids after being irradiated with simulated sunlight, they are removed from the container used for the photothermal experiment, using a pipette, weighed and the water that was evaporated is replaced and the absorbance is measured employing a spectrophotometer. UV-vis (Figure 1). The original spectrum of the nanofluid is compared with the irradiated sample and based on this it can be verified if there were changes.

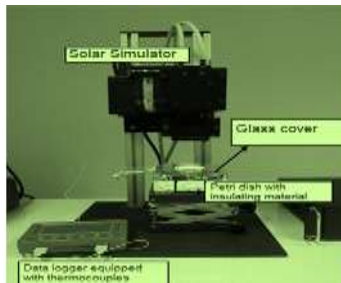


Figure 1. Experimental setup of the photo thermic experiment.

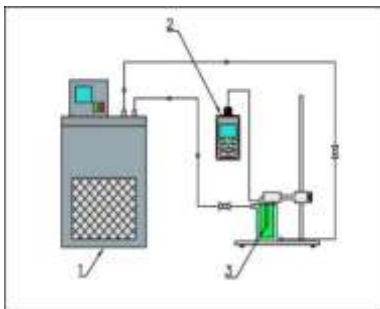


Figure 2. Representation of the assembly used for the measurement of thermal conductivity. (1) Circulating cooling bath, (2), Thermal properties analyzer (3) KS1 sensor,

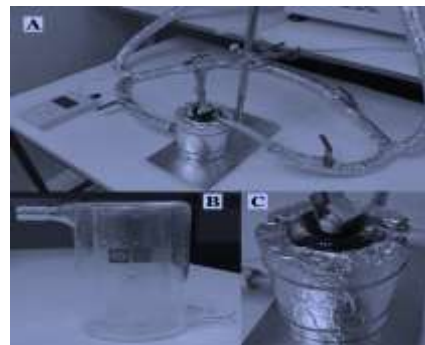


Figure 3. Images of the assembly used to measure thermal conductivity (A) complete assembly, (B) Cup with thermal jacket, (C) Cup with thermal jacket covered with polystyrene insulation covered with aluminum foil

Thermal conductivity measurement

Thermal conductivity measurements were carried out in the Thermal Energy Storage laboratory belonging to the college of Energy Engineering, University POLITEHNICA of Bucharest. For the measurement, a thermal bath was used, the thermal properties analyzer with the KS1 sensor, a glass beaker with a jacket where the refrigerant circulated, and shut-off valves (Figure 2). The fluid to be measured was placed in the glass beaker with a jacket and was thermally isolated through a polystyrene layer covered with aluminum foil (Figure 3). Once the fluid is placed in the jacketed vessel (d), the thermal bath is turned on, setting a coolant temperature at 17°C . Valves (c),

(e) and (g) open and (f) closes. Once the nanofluid reaches equilibrium temperature, around a time of 6 minutes, the valves (c) and (e) are closed to stop the flow of refrigerant towards the vessel containing the substance under study, and the valve (f) so that the refrigerant continues its movement and does not damage the thermal bath pump. The nanofluid is expected to come to rest, approximately 2 minutes. Finally, the measurement of thermal conductivity is performed by using the thermal properties analyzer. The cycle described above is repeated to obtain a series of measurements of the desired property.

RESULTS AND DISCUSSIONS

Characterization

SEM and STEM images were performed to determine the shapes and dimensions of the nanoparticles contained in the nanofluids. The images of the gold nanoparticles are shown in Figure 4 (A) and (B), where it can be seen that they are spherical in shape, have a diameter between 10 and 30 nm and tend to agglomerate with each other. Silver nanoparticles formed by chemical reduction synthesis using sodium citrate are spherical in shape, 20 to 50nm in size, and also tend to bond with each other, Figure 5 (A) and (B). The cubic silver nanofluid is shown in Figure 6 (A) where it can be seen that the particle size is in the range 20 to 70 nm. The image of the copper nanodispersion is shown in Figure 6 (B), where it can be seen that in the center there are a set of particles larger than 70 nm, and in the contours others smaller than 40 nm. The size of the core particles could be attributed to the agglomeration of small nanoparticles.

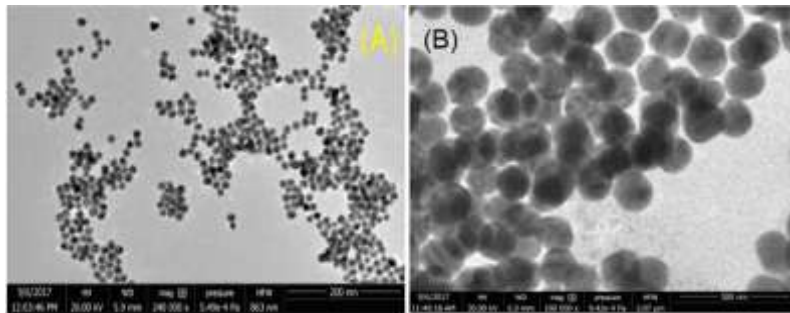


Figure 4. Gold nanofluid (A) STEM image 200 nm; (B) SEM 500 nm image

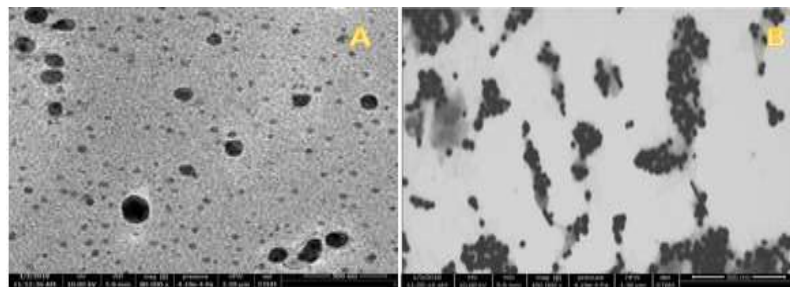


Figure 5. Spherical silver nanofluid (A) 500 nm STEM image; (B) STEM 300 nm image

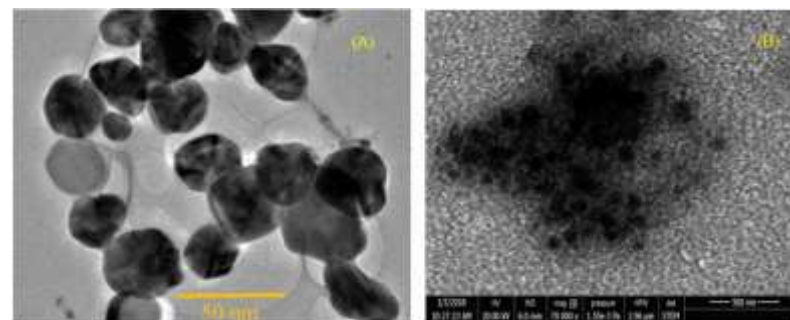


Figure 6. (A) Cubic silver nanofluids TEM image; (B) STEM copper nanofluid image

The high and low oxidation GO nanofluids have existed as the sheets of the former are more compact, but smaller in size. Regarding the silver hybrid fluids with low oxidation GO, it is observed that for the case of *in situ* synthesis, the result was silver nanoparticles with a diameter of 20 - 30 nm deposited uniformly on the surface of GO; while in the case of *ex situ* synthesis, the presence of silver nanoparticles on GO is not observed, which could be attributed to the fact that they are dispersed in the liquid without adhering to the surface of GO. The radiative properties of the nanofluids used were measured using a UV-vis spectrophotometer. For the case of metallic nanodispersions of gold, spherical silver, cubic silver and copper at a concentration of 0.01 wt%, absorption, and transmittance spectra were obtained that are shown in Figure 7 (a-d); where it is observed that these fluids have the ability to absorb light in the visible range, and have plasmons at wavelengths of 527 nm, 430nm, 590 nm and 571 nm for gold, spherical silver, cubic silver, and copper respectively. These results are consistent with that reported by references[15]. While for GO nanofluids with high and low oxidation, plasmons were obtained at wavelengths of 227 nm and 249 nm respectively, Figure 12, which is similar to what was achieved by similar studies[16]. In the case of hybrid GO-Silver nanofluids *in situ* and *ex-situ*, a spectrum was obtained, which can be seen in Figure 13, where it is observed that adding silver nanoparticles to the low-oxidation GO considerably increases the absorption of visible light. It should be noted that for the *in situ* case a displacement of the absorption peak towards the UV was obtained, reaching 400 nm, similar to that reported by [17].

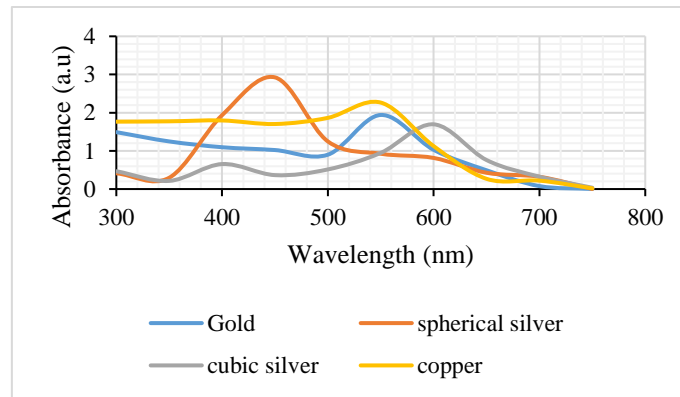


Figure 7. Nanofluid absorbance of (a) gold; (b) spherical silver; (c) cubic silver; and (d) copper

While for the *ex-situ* case the individual peaks of each species are conserved separately. The transmittance of each of the nanofluids is measured and compared with the base fluid that corresponds to deionized water. In Figure 11, a comparison of metallic nanofluids with water is shown, obtaining that all nanofluids obtain a lower transmittance at wavelengths 200 - 1100 nm, which allows concluding that the radiation of these wavelengths is attenuated by to a greater extent due to nanofluids, that is, it is shown that these have greater absorption capacity than the base fluid. In the case of wavelengths between 200 - 550 nm, the gold nanofluid is the one with the lowest transmittance (highest absorption capacity), while for the range 550 - 850 nm, the cubic silver is the one with the lowest transmittance. For the case of GO nanofluids, similar results are obtained compared to water, (Figure 9). For the low oxidation nanofluid, lower transmittance is obtained in most of the spectrum considered, which can be attributed to the greater presence of carbon in said nanofluid, this can be verified by the darker color that the nanofluid acquires (Figure 10). The GO-silver nanofluidic hybrids achieve a lower transmittance than the pure species alone, which allows us to conclude an improvement in absorption when combining both particles (Figure 11).



Figure 10. GO nanofluid (left) low oxidation, (right) high oxidation

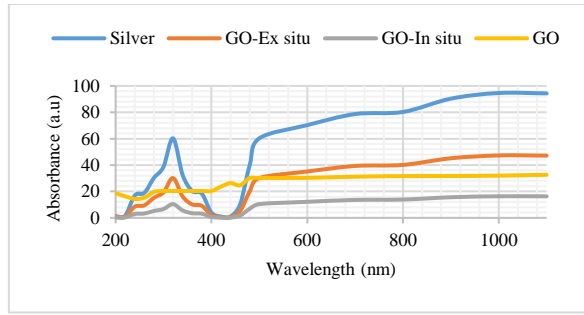


Figure 11. Absorbance of hybrid GO-silver nanofluids prepared by the method: (A) *In-situ*, and (B) *Ex-situ*

Stability of nanofluids

Stability over time

To measure the stability of nanofluids, the optical absorption spectrum of nanofluids is measured once they have been synthesized and after a period of time has elapsed. The metallic nanoparticles such as gold and silver after more than 50 days had elapsed, the spectra showed differences in absorbance of approximately 9% for both gold (Figure 12) and silver, allowing to conclude that they remained stable compared to copper, which later of 8 days had a variation of 52% in its absorption spectrum. These results coincide with the references that state that in the case of gold and silver they remain stable for up to more than 2 months and that the copper nanofluids are highly unstable over time. The stability of the gold and silver nanofluids is due to the fact that during the synthesis sodium citrate is used as a reducing agent, the citrate contains COO⁻ that adheres to the surface of the nanoparticles producing the formation of the double layer which allows the particles repel each other and do not agglomerate. On the other hand, the instability of copper is due to the fact that the nanoparticles are oxidized, gaining mass, which causes sedimentation, as has been reported[18]. The low oxidation GO nanofluid with a mass concentration of 0.005 5% was stored for 85 days and was moderately stable reducing the intensity of the spectrum. Sedimentation is due to the laminar form of GO, which has a greater contact area that facilitates Van der Waals interactions, agglomerating and later sedimentation. In addition, the stability of hybrid nanofluids made up of GO-Silver synthesized using the in situ and ex situ technique is studied. According to the results obtained, it can be concluded that after 21 days the ex situ synthesis gives rise to more stable nanofluids. This could be due to the fact that in the in situ method the GO interferes in the reduction reaction of the silver salt, which would cause a smaller amount of COO⁻ groups to reach the surface of the silver nanoparticles, being less stable because they are it would form a weaker double layer than if it were formed in the reduction reaction without GO.

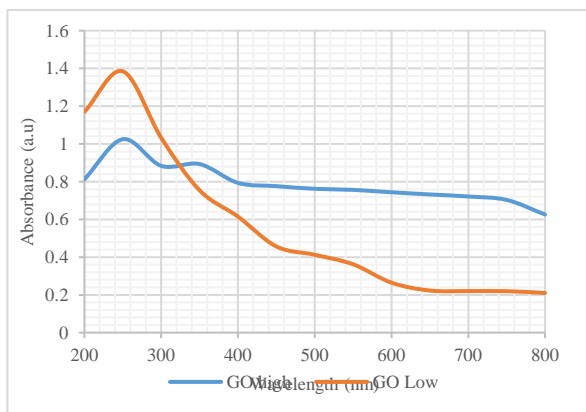


Figure 8. (A) high oxidation GO nanofluid absorbance, and (B) low oxidation

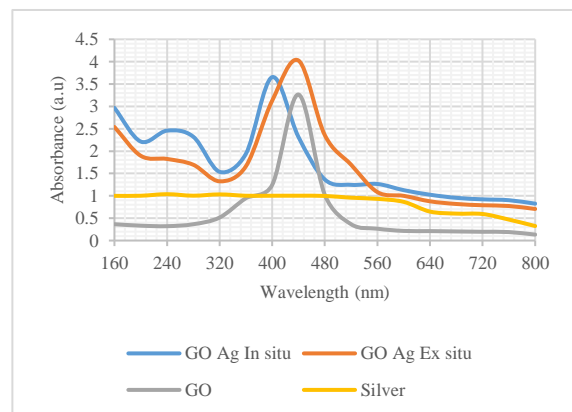


Figure 9. Absorbance of hybrid low oxidation GO nanofluids with silver

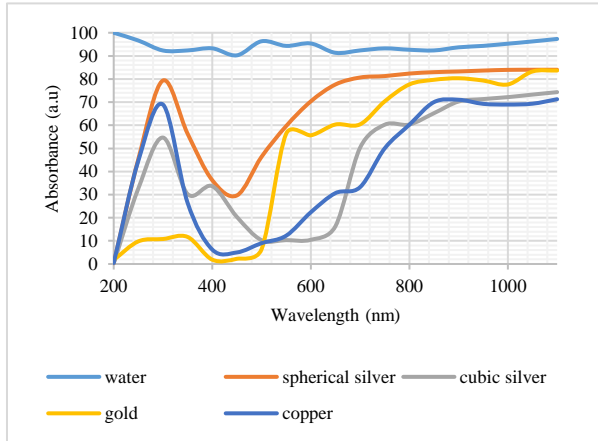


Figure 12. Metallic nanofluid transmittance and its comparison with deionized water

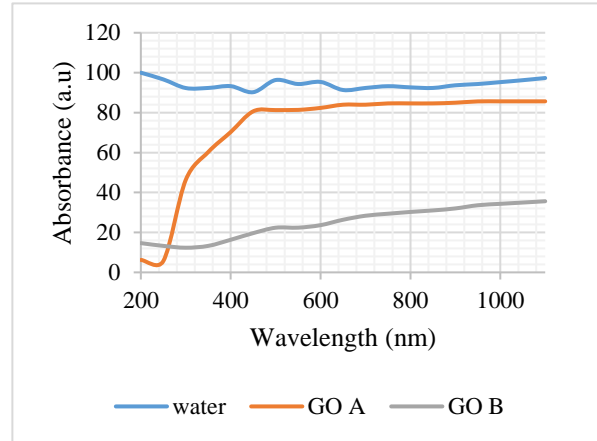


Figure 13. Water and nanofluid transmittance of high oxidation (GO A) and low oxidation (GO B) GO

Stability after a radiation cycle

After the photothermal experiment, where the nanofluids were subjected to periods of simulated solar radiation of 50 minutes, a UV spectrum was performed *vis* the nanofluids of gold (Figure 18), spherical silver (Figure 22), cubic silver (Figure 20), copper (Figure 21), GOB (Figure 22) and GOB with a silver (Figure 23). It should be noted that in all nanofluids there was a reduction in the intensity of the absorption spectrum except in nanofluids where spherical silver was involved (both for pure and hybrid fluid. In the case of gold, the reduction could be due to oxidation of a part of the nanoparticles, and reducing the number of these reduces the absorption capacity of the nanofluid. Another cause may be the agglomeration of nanoparticles caused by subjecting the nanofluid to heating, this was reported by Otanicar where it heated nanofluids and performed nanoparticle size measurements obtaining an increase in it[19]. However, it should be noted that in this study the gold nanofluids proved to be highly stable and present increases in their transmittance that turned out to be negligible compared to the other nanofluids tested, but Unlike the present work, and The heating of the nanofluid was carried out by a thermal plate, so the use of simulated solar radiation is a more extreme operating condition, so it would be necessary to perform nanoparticle size measurements to verify if the reduction in absorbance is due to this factor. . However, according to what has been reported by studies of gold nanoparticle sizes, the UV-vis spectrum must be more intense and acute for there to be an increase in particle size or agglomeration, and in the results obtained, the opposite occurred. Due to this background, an agglomeration of gold nanoparticles would not be feasible. Figure 13 also shows a normalized graph of the absorbance spectrum of gold where it can be seen that there is a negligible shift in the peak of the curve.

For the case of spherical silver (Figure 19) and for the hybrid nanofluid GOB-silver (Figure 20) an increase in the intensity of the absorbance is observed, there was no greater displacement of the peak according to the normalized graph. It should also be noted that a color change from yellow to gray is observed in the case of the silver nanofluid after two cycles of irradiation. Increased absorbance and color change were not reported in the reviewed literature, and analysis is required to find the cause of this phenomenon. However, photothermic experiments are performed to see if this change has any effect on their performance. In the case of cubic silver (Figure 20), a reduction in absorbance intensity is observed without peak displacement, which may be due to agglomeration of silver particles due to heating, according to that reported by Otanicar, where the nanofluid of silver on which I perform heating tests increased its transmittance[20]. For copper and GOB nanofluids, Figure 21 and Figure 22 respectively show a drastic reduction in the intensity of absorbance after subjecting these nanofluids to periods of solar radiation. It should be noted that when removing these nanofluids from the container where the photothermic experiments were carried out, it was observed that they had sedimented nanoparticles, which could not be completely recovered, so the change in the spectrum is due to the fact that the samples analyzed in the spectrophotometer they had fewer nanoparticles.

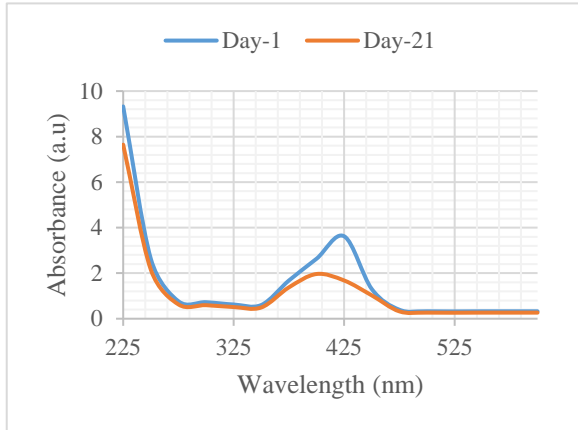


Figure 16. Time stability of Ag-GO nanofluid (low oxidation) prepared *in situ* at a concentration of 0.005 wt%

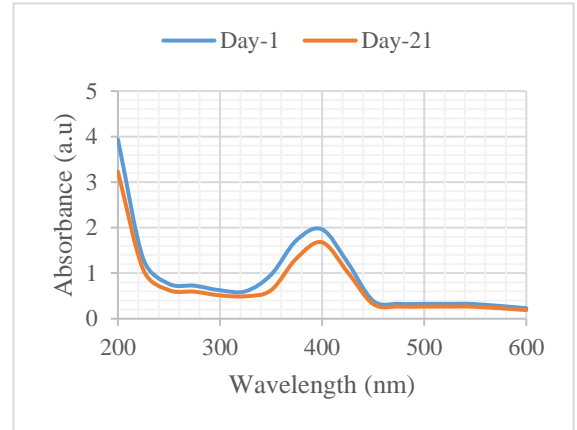


Figure 17. Ag-GO nanofluid time stability (low oxidation) prepared *ex-situ* at a concentration of 0.005 wt%

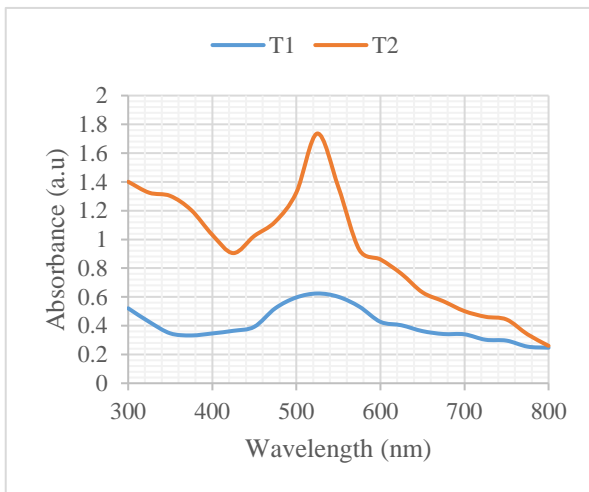


Figure 18. Effect of solar radiation on the absorbance of gold nanofluid before (T1) and after being subjected to radiation (T2)

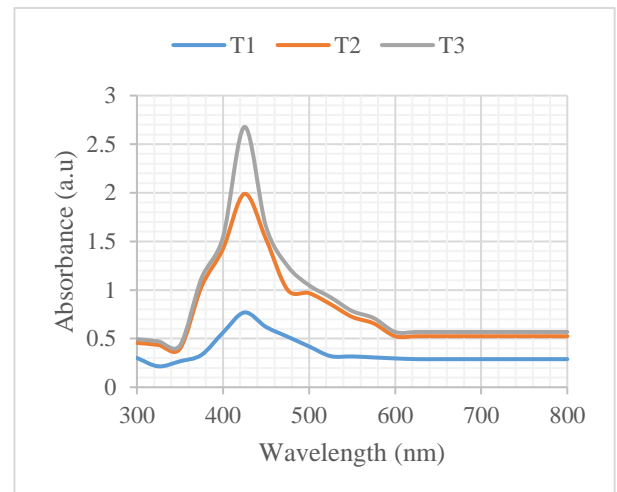


Figure 19. Effect of solar radiation on spherical silver nanofluid absorbance before (T1) and after being subjected to radiation (T2) and then subjected to the second period of radiation (T3)

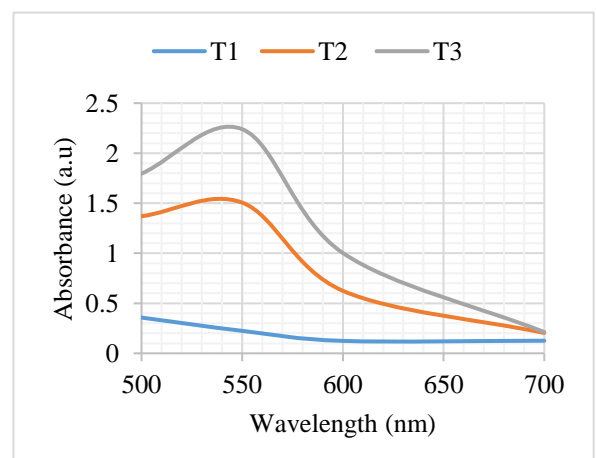
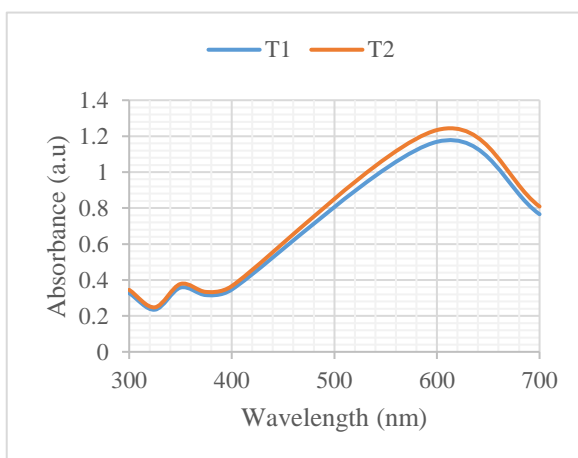


Figure 20. Effect of solar radiation on the absorbance of cubic silver nanofluid before (T1) and after being subjected to radiation (T2)

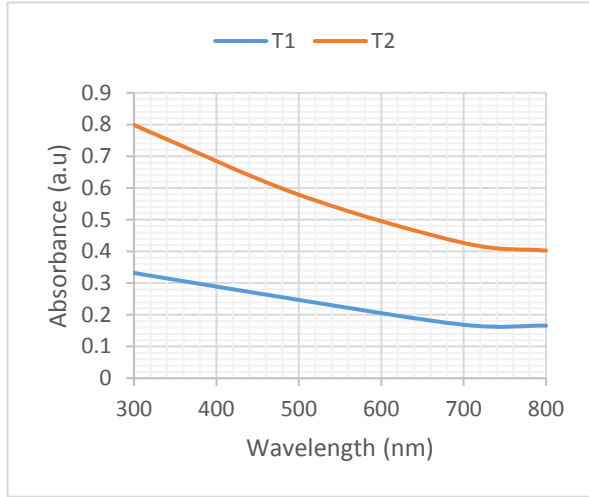


Figure 22. Effect of solar radiation on the absorbance of low oxidation GO nanofluid before (T1) and after being subjected to radiation (T2)

Figure 21. Effect of solar radiation on the absorbance of copper nanofluid (T1) and after being subjected to radiation (T2) and then a second radiation period (T3) is applied

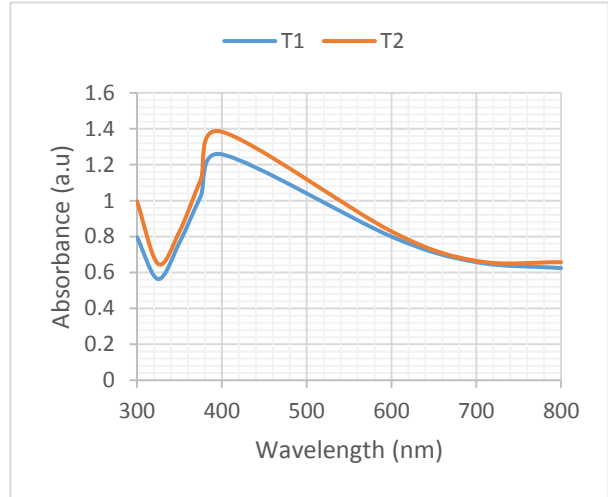


Figure 23. Effect of solar radiation on GO nanofluid absorbance (low oxidation) with in-situ silver before (T1) and after being subjected to radiation (T2)

Thermal conductivity

The conductivity of the nanofluids used was measured at a temperature of 18°C and using a concentration of 0.01 w% (Figure 24). Nanofluids are observed to have an improvement in thermal conductivity compared to deionized water. However, when performing a statistical test using the mean hypothesis test using t-student, given the size of the samples for each nanofluid, which was less than 12, it was obtained that the differences between the values using a confidence level of 95% It was obtained that the improvement in thermal conductivity is only significant for gold nanofluids, GO high oxidation (GO-A) and GO low oxidation (GO-B) as shown in Figure 25, but it cannot be established that it exists a significant difference between them. From the results obtained, the non-significant improvement of the silver nanofluid that n coincides with the reference[21] is surprising, this could have occurred due to the high dispersion of the experimental values obtained, while the low conductivity of copper could be due to the high instability of said nanofluid since the test was carried out one day after synthesis and also due to the high dispersion of the experimental results. The results obtained by the different GOs were not expected either, because the most oxidized one is expected to have a lower thermal conductivity, but the high oxidation GO is in agreement with the value obtained by [1]who obtained an 8% improvement at 30°C and in this study a 5.7% improvement was obtained at 18 ° C and the same concentration and using the same measuring device.

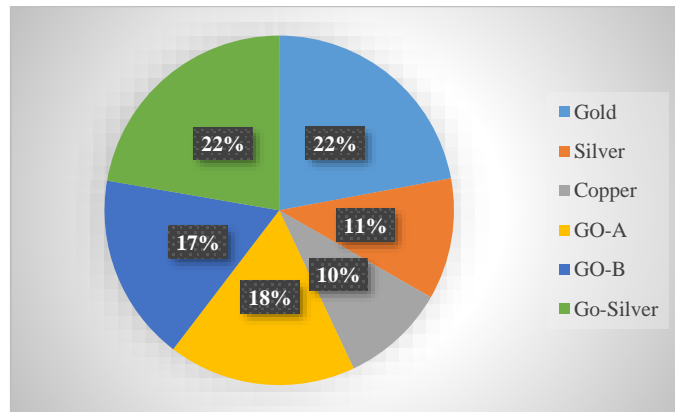


Figure 24. Percentage of improvement in thermal conductivity of different nanofluids for deionized water at 18 °C and using a concentration of 0.01 wt%

Photo thermic experiments

a) Nanoparticle type effect: To study the effect of the nanoparticle type, it was carried out using a concentration of 0.01% in mass percentage, and the results are shown in Figure 25 for the metallic nanofluids and the GO nanofluids. In the case of metallic nanofluids, it is observed that they reach 5°C of difference with respect to water once they reach a steady state. This change may be induced by the increase in effective thermal conductivity of the dispersion in nanoparticles of materials with high thermal conductivity, by growing the thermal conduciveness of the heat generated by radiation absorption in a nanofluid more quickly. In the visible spectrum of metal nanofluids, the increased equilibrium temperature can also be due to a very high absorption efficiency relative to the lowest water. Comparing each of the nanoparticles used, the gold nanofluid is the one with the highest absorption capacity in the visible range, (Figure 8), and consequently, there should be a difference between the temperature profiles reached by the metals, given that light visible is around 50% of solar radiation. This contradiction in the results was discussed by [18] where he concluded that performing UV vis spectrophotometry is not a very accurate parameter to predict the photothermal conversion of nanofluids since UV-vis photometry shows the selectivity of the nanoparticle to absorb radiation of a certain wavelength, and not the capacity of the nanoparticle to transform solar radiation into thermal energy, which would allow to conclude that the plasmons (or absorbance peaks) of each type of metallic nanoparticle would not make a difference in the conversion of radiation into heat. According to a study carried out by Chen (2011), where he used a numerical study to predict the behavior of different types of nanofluids using equal conditions, he obtained that there is no difference between gold and silver in terms of their thermal performance, so the results obtained would be consistent. Although copper had results similar to those of gold and silver, it must be considered that the stability of copper was 3 days compared to the other metallic particles, which was months, this would allow concluding that the equilibrium temperature results achieved by copper nanofluids would fluctuate dramatically over time. Regarding the results obtained with the GO of different degrees of oxidation (Figure 26), it was obtained that the GO of low oxidation (GOB) obtained a difference of 6°C for water and 3°C with respect to GO high degree of oxidation (GOA), both differences were found to be statistically significant using a confidence level of 95%. This makes sense because the percentage of carbon that the GOB has is higher than the oxidized, because of this the GOB has better optics, according to UV-Vis spectrophotometry, compared to GOA and the increase in oxygen content drastically reduces the thermal conductivity. It is important to note that GOB, as it has fewer hydrophilic functional groups, costs more to disperse in water and sediments before GOA. Analyzing all the results by species, it was obtained that there is no significant difference between metallic nanofluids and those of low oxidation GO, therefore explanations related to plasmonic resonance of metallic nanofluids would not be applicable in isolation in this work because the GO fluid that does not belong to said group obtains a similar equilibrium temperature compared to the metallic nanofluids. The high equilibrium temperature reached by the GOB could be attributed, in part, to its low transmittance in the range 200 - 1100 nm reaching a maximum of 40%, (Figure 13), while gold from 560 nm reduces its absorption drastically, (Figure 12); and this would offset the eventual plasmonic effect of the metallic nanoparticles. It should be noted that if the thermal conductivity results obtained are considered, it can be seen that the improvement in thermal conductivity obtained with respect to water would explain the higher equilibrium temperature reached. However, as differences are so similar between nanofluids, it would justify the similar result in terms of equilibrium temperature, but it would not explain it completely because the high oxidation GO obtains a similar value to the low one in terms of thermal conductivity and different in the case of the equilibrium temperature obtained in the photothermal experiment. An important aspect for the choice of nanofluids would be the cost of production, due to the results obtained for the same concentration of nanofluids and the same irradiance, it is convenient to choose the one with the lowest cost such as the one with low oxidation GO, while the one with the highest cost it would be the gold one due to the high cost of the gold salt or chloroauric acid reagent.

b) Height effect of nanofluid: For the nanofluids that presented the best results in the previous test, a test was carried out using a greater quantity of nanofluid to increase the penetration height of solar radiation (assembly B) and study possible shielding effects of the nanoparticles found in the upper area of the fluid. As expected, the temperatures reached by the fluids were lower than that of the assembly with a lower fluid height, this is since the heated mass was increased. However, it was obtained that the low oxidation GO removes a difference of 1.5°C and 5.5°C with respect to the metallic nanofluids and water respectively, while the metallic ones obtain a difference of 4°C with respect to the Water. The thermal improvement obtained by nanofluids with respect to

water is slightly lower in the assembly with the highest fluid height, but this difference is not conclusive since it is in the experimental error margin of 1°C .

c) Concentration effect: To study the effect of concentration of nanoparticles, photothermal experiments of metallic nanofluids and GO (high and low oxidation) were performed, (Figure 25, 26, and Figure 27 respectively. For metallic nanofluids, an increase in equilibrium temperature was obtained with increasing concentration, because increasing the number of nanoparticles increases the thermal conductivity of the fluid and increases the absorption capacity. However, this increase decreases with higher concentration, as can be seen at concentrations of $0.02\text{ wt}\%$, as can be seen in Figure 30. The latter can be attributed to the fact that at a certain concentration the nanoparticles on the surface of the fluid prevent the passage of radiation, not allowing the heating of the interior particles. Furthermore, when the nanofluids surface temperature is higher, heat losses to the environment increase. In the case of GO nanofluids, trends similar to metallic ones were obtained, as seen in Figure 30. It is also important to note that the nanofluid that reached the greatest difference with respect to water was the GOB at a mass concentration of 0.02% that obtained 7.5°C above the water, that is, a 25% improvement in the equilibrium temperature.

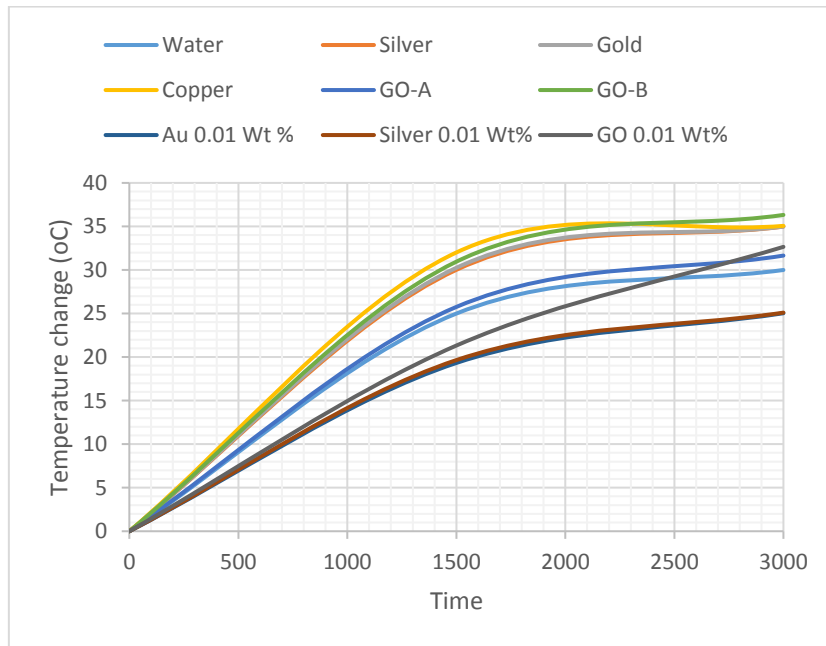


Figure 25. Photothermal experiment results for metallic nanofluids at a mass concentration of 0.01% , GO nanofluids at a mass concentration of 0.01% and Temperature profile of photothermal experiment using a fluid height of 13 mm

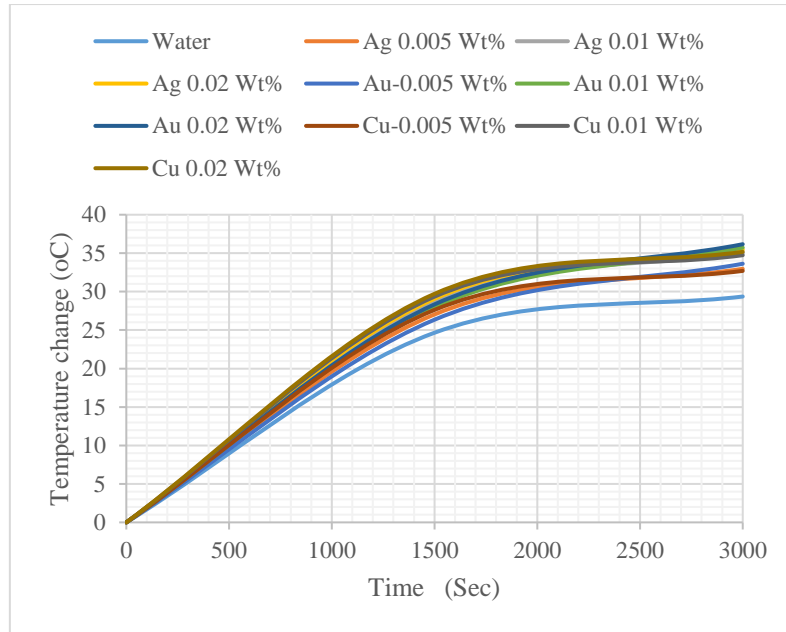


Figure 26. Photothermic experiment metallic nanofluids different concentrations: gold, silver, and copper

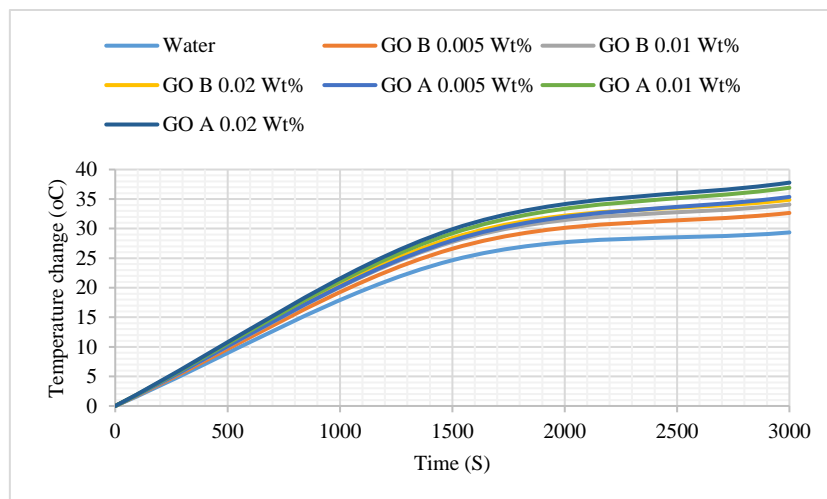


Figure 27. Nanofluid photothermal experiment of GO different concentrations: (A) low oxidation, and (B) high oxidation

d) Nanoparticle shape effect: Silver nanofluids at a mass concentration of 0.01% containing spherical and cubic shaped nanoparticles were used to study the effect of nanoparticle shape. The results obtained are shown in Figure 28. It is observed that the thermal performance of the fluid is similar, being that of spherical nanoparticles the one that has the best performance, reaching a difference of 2°C with respect to that of cubes, not being a significant difference. This result was not expected due to the difference in the visible light absorption spectrum and the size of the spherical silver nanoparticles ($20 - 50 \text{ nm}$) which are smaller than the cubic ones (sizes greater than 40 nm) and as a consequence the former they should have a higher thermal conductivity due to the greater surface area and greater radiation absorption capacity according to that reported by [8]; Therefore, it can be concluded for this work that the effect of shape and size would not have a preponderant role in the equilibrium temperature reached by the nanofluid.

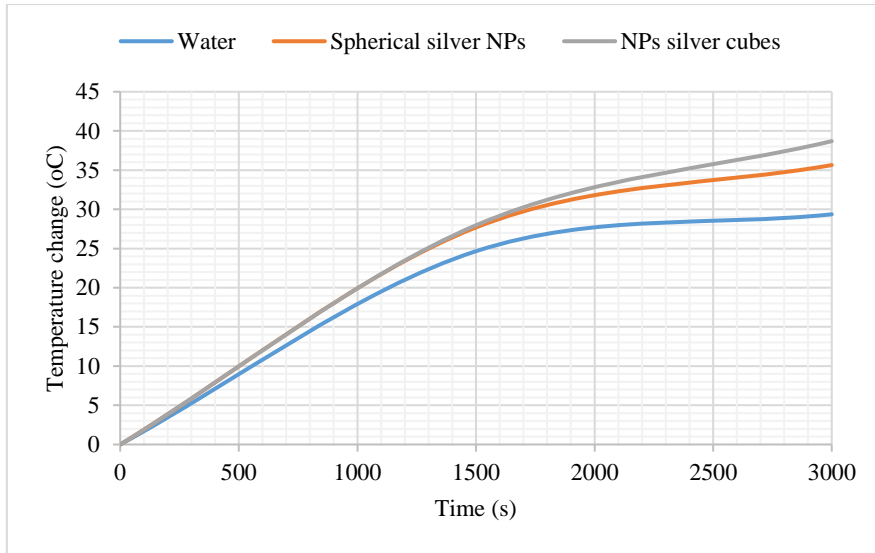


Figure 28. Effect of silver nanoparticle shape in the photothermal experiment

e) Hybrid nanofluids: To study the effect of hybrid nanofluids, photothermal experiments were carried out using nanofluids manufactured *ex-situ* (Figure 29 and *in-situ*) obtaining for both cases very similar yields to each nanofluid separately and not obtaining an expected synergistic effect according to those reported by other researchers who achieved improvements using GO with gold, obtaining an improvement of $10\text{ }^{\circ}\text{C}$ and $3\text{ }^{\circ}\text{C}$ compared to water and with pure GO nanofluid using an irradiance of 700 W/m^2 . However, in this study 5 times, higher concentrations of GO and more than 100 times higher concentrations of gold nanoparticles were used. With the result obtained in this experiment, it is shown that at low concentrations of GO and silver there are no synergistic effects of the union of these hybrid nanoparticles, both in the *in-situ* and *ex-situ* preparation.



Figure 29. Photothermal experiment results for GOB-silver nanofluids prepared in form Ex-situ using GOB and Ag at a concentration of 0.005 wt%, and In-situ using a concentration of 0.01 wt%

Photo thermic experiments with already irradiated nanofluids

The second cycle of radiation was applied to the most stable nanofluids, silver and gold, after cooling after the first cycle, to be able to observe if there are changes in their photothermal performance, these results can be observed in Figure 30 for silver and the case of gold. As can be seen in both cases, during both radiation cycles a very similar temperature profile is observed despite the changes in the absorbance of the nanofluids shown in Figure 18 for the case of gold and Figure 19 for silver. This difference would allow to rule out the hypothesis that any change in the absorption spectrum in the UV-visible range alters the temperature profiles reached by the nanofluids and the changes in the spectra that would affect the temperature profile reached in the photo thermal experiments would be those that are produced by the sedimentation of particles. With the results obtained in this section, the suspicions raised regarding the reduction of the number of gold nanoparticles can be eliminated, given that the temperature profile is maintained. Nor would it be feasible for particle agglomeration to exist, since if it did occur, the temperature profile should be modified due to the change in size according to what was reported by [8] who obtained different temperature profiles when they modified the size of gold nanoparticles. It would be interesting to increase the radiation cycles to know if there is a limitation of cycles for which the nanofluid reduces its performance.

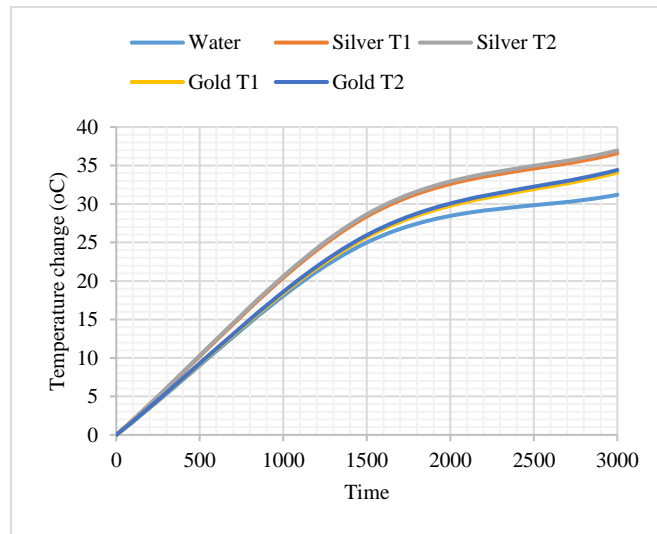


Figure 30. Photothermal experiments during two cycles of solar radiation for nanofluids of silver and gold, where T1 corresponds to the fluid irradiated for the first time and T2 to a second irradiation

CONCLUSIONS

Nanofluids were synthesized using water-based fluid and nanoparticles of metals (gold, silver, and copper), graphene oxide (high and low oxidation), and hybrid nanoparticles composed of graphene oxide and silver. The synthesized nanofluids were characterized by electron microscopy and UV-visible spectroscopy images. Nanofluids have a high absorption capacity in the UV-visible spectrum compared to deionized water. They have a higher thermal conductivity compared to the base fluid. In photothermal experiments, the addition of nanoparticles to the base fluid increases the equilibrium temperature compared to deionized water. In the case of metal nanoparticles and low oxidation graphene oxide, a differentiating effect of the material used is not observed at the same irradiance and concentration, although they present different radiative properties such as absorbance and transmittance and different thermal conductivities, this means that there would not be a direct relationship between the radiative properties and the equilibrium temperature reached, and the properties such as absorbance or transmittance just to know in which range of the spectrum the nanofluid absorbs radiation. Regarding the effect of concentration, it was obtained that the higher the concentration the equilibrium temperature increases, but the growth is decreasing, reaching a point where the addition of nanoparticles does not improve the equilibrium temperature. No effect is observed between cubic and spherical silver nanoparticles in the photothermal experiment. Increasing the fluid height reduces the equilibrium temperature of all nanofluids, but maintains the difference between the temperatures reached by the nanofluids and the base fluid. The degree of oxidation of graphene oxide alters the radiative properties, and the equilibrium temperature reached in the photothermal experiment, being the low oxidation the one that reaches the highest equilibrium temperature in the photothermal experiment. Nanofluids subjected to solar radiation show changes in their radiative properties. In the case of gold and silver nanofluids already subjected to radiation, they were again subjected to a photothermal experiment

obtaining the same equilibrium temperature reached by the nanofluid irradiated for the first time, which allows concluding that the changes observed in the UV-visible spectrum do not affect the equilibrium temperature reached by the nanofluids. The hybrid nanofluid of low oxidation GO and silver does not present significant improvements in the equilibrium temperature in the photothermic experiment with respect to each species, in terms of thermal conductivity there are also no improvements with respect to the components separately.

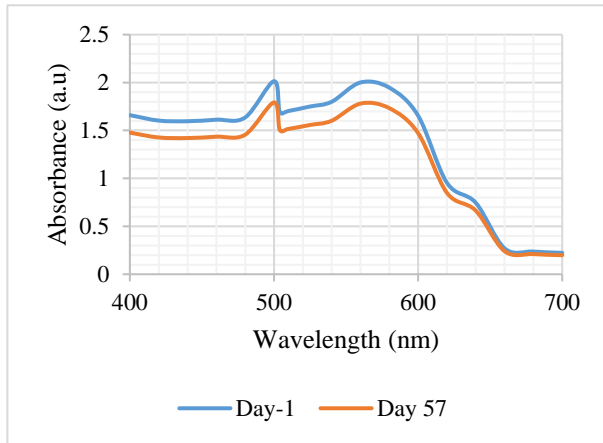


Figure 4.15. Gold nanofluid stability over time

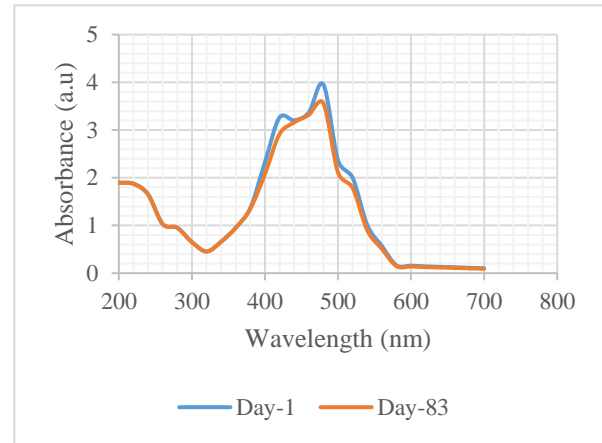


Figure 4.16. Gold nanofluid time stability

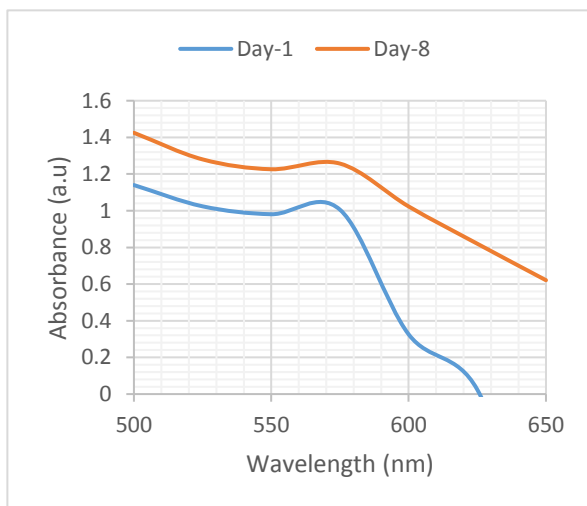


Figure 4.17. Time stability of copper nanofluid

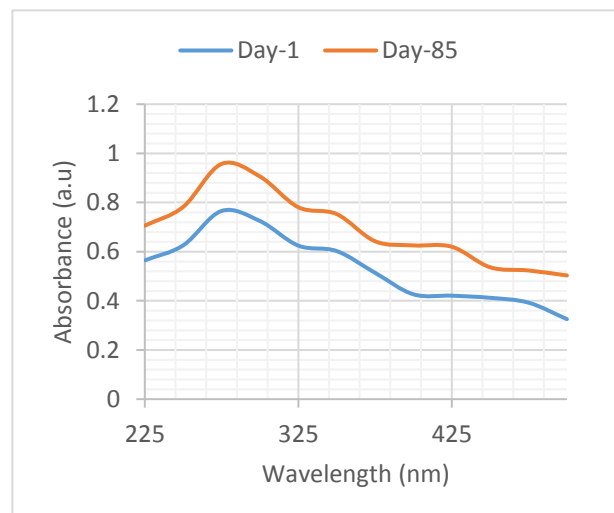


Figure 4.18. Time stability of low oxidation GO nanofluids at a concentration of 0.05 wt%

REFERENCES

- [1] S. Akilu, K. V. Sharma, A. T. Baheta, and R. Mamat, "A review of thermophysical properties of water based composite nanofluids," *Renew. Sustain. Energy Rev.*, vol. 66, pp. 654–678, 2016, doi: 10.1016/j.rser.2016.08.036.
- [2] S. U. S. Choi, "Enhancing thermal conductivity of fluids with nanoparticles," *Am. Soc. Mech. Eng. Fluids Eng. Div. FED*, vol. 231, 1995, pp. 99–105, 1995.
- [3] H. E. Patel, T. Sundararajan, and S. K. Das, "An experimental investigation into the thermal conductivity enhancement in oxide and metallic nanofluids," *J. Nanoparticle Res.*, vol. 12, no. 3, pp. 1015–1031, 2010, doi: 10.1007/s11051-009-9658-2.
- [4] A. Lenert, "Solar Thermal Heat Transfer Fluids," *Annu. Rev. Heat Transf.*, vol. 15, pp. 93–129, 2012, doi: 10.1615/AnnualRevHeatTransfer.2012004122.

- [5] W. Chamsa-ard, S. Brundavanam, C. C. Fung, D. Fawcett, and G. Poinern, *Nanofluid types, their synthesis, properties and incorporation in direct solar thermal collectors: A review*, vol. 7, no. 6, 2017.
- [6] N. K. Gupta, A. K. Tiwari, and S. K. Ghosh, *Heat transfer mechanisms in heat pipes using nanofluids – A review*, vol. 90. Elsevier Inc., 2018.
- [7] A. Ijam and R. Saidur, “Nanofluid as a coolant for electronic devices (cooling of electronic devices),” *Appl. Therm. Eng.*, vol. 32, no. 1, pp. 76–82, 2012, doi: 10.1016/j.applthermaleng.2011.08.032.
- [8] M. Y. Al Shdaifat, R. Zulkifli, K. Sopian, and A. A. Salih, “Thermal and hydraulic performance of CuO/water nanofluids: A review,” *Micromachines*, vol. 11, no. 4, 2020, doi: 10.3390/MI11040416.
- [9] T. P. Otanicar, P. E. Phelan, R. S. Prasher, G. Rosengarten, and R. A. Taylor, “Nanofluid-based direct absorption solar collector,” *J. Renew. Sustain. Energy*, vol. 2, no. 3, 2010, doi: 10.1063/1.3429737.
- [10] A. Bhattad and J. Sarkar, “Effects of nanoparticle shape and size on the thermohydraulic performance of plate evaporator using hybrid nanofluids,” *J. Therm. Anal. Calorim.*, 0123456789, 2019, doi: 10.1007/s10973-019-09146-z.
- [11] N. I. Zaaba, K. L. Foo, U. Hashim, S. J. Tan, W. W. Liu, and C. H. Voon, “Synthesis of Graphene Oxide using Modified Hummers Method: Solvent Influence,” *Procedia Eng.*, vol. 184, pp. 469–477, 2017, doi: 10.1016/j.proeng.2017.04.118.
- [12] K. Ranoszek-Soliwoda *et al.*, “The role of tannic acid and sodium citrate in the synthesis of silver nanoparticles,” *J. Nanoparticle Res.*, vol. 19, no. 8, 2017, doi: 10.1007/s11051-017-3973-9.
- [13] A. Khan, A. Rashid, R. Younas, and R. Chong, “A chemical reduction approach to the synthesis of copper nanoparticles,” *Int. Nano Lett.*, vol. 6, no. 1, pp. 21–26, 2016, doi: 10.1007/s40089-015-0163-6.
- [14] S. Chandrasekaran *et al.*, “Recent advances in metal sulfides: From controlled fabrication to electrocatalytic, photocatalytic and photoelectrochemical water splitting and beyond,” *Chem. Soc. Rev.*, vol. 48, no. 15, pp. 4178–4280, 2019, doi: 10.1039/c8cs00664d.
- [15] N. T. Tam *et al.*, “Carbon nanomaterial-based nanofluids for direct thermal solar absorption,” *Nanomaterials*, vol. 10, no. 6, pp. 1–39, 2020, doi: 10.3390/nano10061199.
- [16] L. Huang, H. Yang, Y. Zhang, and W. Xiao, “Study on Synthesis and Antibacterial Properties of Ag NPs/GO Nanocomposites,” *J. Nanomater.*, vol. 2016, 2016, doi: 10.1155/2016/5685967.
- [17] E. C. Okonkwo, I. Wole-Osho, I. W. Almanassra, Y. M. Abdullatif, and T. Al-Ansari, *An updated review of nanofluids in various heat transfer devices*, March. Springer International Publishing, 2020.
- [18] J. Walshe, P. M. Carron, C. McLoughlin, S. McCormack, J. Doran, and G. Amarandei, “Nanofluid development using silver nanoparticles and organic-luminescent molecules for solar-thermal and hybrid photovoltaic-thermal applications,” *Nanomaterials*, vol. 10, no. 6, pp. 1–25, 2020, doi: 10.3390/nano10061201.
- [19] L. Godson, K. Deepak, C. Enoch, B. R. Jefferson Raja, and B. Raja, “Heat transfer characteristics of silver/water nanofluids in a shell and tube heat exchanger,” *Arch. Civ. Mech. Eng.*, vol. 14, no. 3, pp. 489–496, 2014, doi: 10.1016/j.acme.2013.08.002.
- [20] J. Chen, W. Chen, D. Song, B. Lai, Y. Sheng, and L. Yan, “The solvent-free mechanochemical synthesis of mildly oxidized graphene oxide and its application as a novel conductive surfactant,” *New J. Chem.*, vol. 43, no. 18, pp. 7057–7064, 2019, doi: 10.1039/c9nj00529c.
- [21] H. Zhang, H. J. Chen, X. Du, and D. Wen, “Photothermal conversion characteristics of gold nanoparticle dispersions,” *Sol. Energy*, vol. 100, pp. 141–147, 2014, doi: 10.1016/j.solener.2013.12.004.